Measurement of the Q^2 Dependence of the Deuteron Spin Structure Function g_1 and its Moments at Low Q^2 with CLAS

K. P. Adhikari,[1,2,3] A. Deur,[2,4,*] L. El Fassi,[1,3] H. Kang,[5] S. E. Kuhn,[1] M. Ripani,[6] K. Slifer,[4,7] X. Zheng,[4] S. Adhikari,[8] Z. Akbar,[9] M. J. Amaryan,[1] H. Avakian,[2] J. Ball,[10] I. Balossino,[11] L. Barion,[11] M. Battaglieri,[6] I. Bedlinskiy,[12] A. S. Biselli,[13] P. Bosted,[14] W. J. Briscoe,[15] J. Brock,[2] S. Bültmann,[1] V. D. Burkert,[2] F. Thanh Cao,[16] C. Carlin,[2] D. S. Carman,[2] A. Celentano,[6] G. Charles,[1] J.-P. Chen,[2] T. Chetry,[17] S. Choi,[5] G. Ciullo,[11] L. Clark,[18] P. L. Cole,[19,2] M. Contalbrigo,[11] V. Crede,[9] A. D'Angelo,[20,21] N. Dashyan,[22] R. De Vita,[6] E. De Sanctis,[23] M. Defurne,[10] C. Djalali,[24] G. E. Dodge,[1] V. Drozdov,[6,25] R. Dupre,[26] H. Egiyan,[2,7] A. El Alaoui,[27] L. Elouadrhiri,[2] P. Eugenio,[9] G. Fedotov,[17,25] A. Filippi,[28] Y. Ghandilyan,[22] G. P. Gilfoyle,[29] E. Golovatch,[25] R. W. Gothe,[24] K. A. Griffioen,[14] M. Guidal,[26] N. Guler,[1] L. Guo,[8,2] K. Hafidi,[30] H. Hakobyan,[27,22] C. Hanretty,[2] N. Harrison,[2] M. Hattawy,[30] D. Heddle,[31,2] K. Hicks,[17] M. Holtrop,[7] C. E. Hyde,[1] Y. Ilieva,[24,15] D. G. Ireland,[18] E. L. Isupov,[25] D. Jenkins,[32] H. S. Jo,[26] S. C. Johnston,[30] K. Joo,[16] S. Joosten,[33] M. L. Kabir,[3] C. D. Keith,[2] D. Keller,[4] G. Khachatryan,[22] M. Khachatryan,[1] M. Khandaker,[34,19] W. Kim,[35] A. Klein,[1] F. J. Klein,[36] P. Konczykowski,[10] K. Kovacs,[4] V. Kubarovsky,[2,37] L. Lanza,[20] P. Lenisa,[11] K. Livingston,[18] E. Long,[7] I. J. D. MacGregor,[18] N. Markov,[16] M. Mayer,[1] B. McKinnon,[18] D. G. Meekins,[2] C. A. Meyer,[38] T. Mineeva,[27] M. Mirazita,[23] V. Mokeev,[2,25] A. Movsisyan,[11] C. Munoz Camacho,[26] P. Nadel-Turonski,[2,15] G. Niculescu,[39,17] S. Niccolai,[26] M. Osipenko,[6] A. I. Ostrovidov,[9] M. Paolone,[33] L. Pappalardo,[40,11] R. Paremuzyan,[7] K. Park,[2,35] E. Pasyuk,[2,41] D. Payette,[1] W. Phelps,[8] S. K. Phillips,[7] J. Pierce,[4] O. Pogorelko,[12] J. Poudel,[1] J. W. Price,[42] Y. Prok,[1,4] D. Protopopescu,[18] B. A. Raue,[8,2] A. Rizzo,[20,21] G. Rosner,[18] P. Rossi,[2,23] F. Sabatié,[10] C. Salgado,[34] R. A. Schumacher,[38] Y. G. Sharabian,[2] T. Shigeyuki,[4] A. Simonyan,[26] Iu. Skorodumina,[24,25] G. D. Smith,[43] N. Sparveris,[33] D. Sokhan,[18] S. Stepanyan,[2] I. I. Strakovsky,[15] S. Strauch,[24] V. Sulkosky,[14] M. Taiuti,[6,44] J. A. Tan,[35] M. Ungaro,[2,37] E. Voutier,[26] X. Wei,[2] L. B. Weinstein,[1] J. Zhang,[4,1] and Z. W. Zhao[1,24]

(CLAS Collaboration)

[1]*Old Dominion University, Norfolk, Virginia 23529, USA*
[2]*Thomas Jefferson National Accelerator Facility, Newport News, Virginia 23606, USA*
[3]*Mississippi State University, Mississippi State, Mississippi 39762-5167, USA*
[4]*University of Virginia, Charlottesville, Virginia 22901, USA*
[5]*Seoul National University, Seoul, Korea*
[6]*INFN, Sezione di Genova, 16146 Genova, Italy*
[7]*University of New Hampshire, Durham, New Hampshire 03824-3568, USA*
[8]*Florida International University, Miami, Florida 33199, USA*
[9]*Florida State University, Tallahassee, Florida 32306, USA*
[10]*IRFU, CEA, Universit'e Paris-Saclay, F-91191 Gif-sur-Yvette, France*
[11]*INFN, Sezione di Ferrara, 44100 Ferrara, Italy*
[12]*Institute of Theoretical and Experimental Physics, Moscow, 117259, Russia*
[13]*Fairfield University, Fairfield, Connecticut 06824, USA*
[14]*College of William and Mary, Williamsburg, Virginia 23187-8795, USA*
[15]*The George Washington University, Washington, DC 20052, USA*
[16]*University of Connecticut, Storrs, Connecticut 06269, USA*
[17]*Ohio University, Athens, Ohio 45701, USA*
[18]*University of Glasgow, Glasgow G12 8QQ, United Kingdom*
[19]*Idaho State University, Pocatello, Idaho 83209, USA*
[20]*INFN, Sezione di Roma Tor Vergata, 00133 Rome, Italy*
[21]*Universita' di Roma Tor Vergata, 00133 Rome Italy*
[22]*Yerevan Physics Institute, 375036 Yerevan, Armenia*
[23]*INFN, Laboratori Nazionali di Frascati, 00044 Frascati, Italy*
[24]*University of South Carolina, Columbia, South Carolina 29208, USA*
[25]*Skobeltsyn Institute of Nuclear Physics, Lomonosov Moscow State University, 119234 Moscow, Russia*
[26]*Institut de Physique Nucléaire, CNRS/IN2P3 and Université Paris Sud, Orsay, France*
[27]*Universidad Técnica Federico Santa María, Casilla 110-V Valparaíso, Chile*
[28]*INFN, Sezione di Torino, 10125 Torino, Italy*
[29]*University of Richmond, Richmond, Virginia 23173, USA*

0031-9007/18/120(6)/062501(7)

[30]Argonne National Laboratory, Argonne, Illinois 60439, USA
[31]Christopher Newport University, Newport News, Virginia 23606, USA
[32]Virginia Tech, Blacksburg, Virginia 24061-0435, USA
[33]Temple University, Philadelphia, Pennsylvania 19122, USA
[34]Norfolk State University, Norfolk, Virginia 23504, USA
[35]Kyungpook National University, Daegu 41566, Republic of Korea
[36]Catholic University of America, Washington, DC 20064, USA
[37]Rensselaer Polytechnic Institute, Troy, New York 12180-3590, USA
[38]Carnegie Mellon University, Pittsburgh, Pennsylvania 15213, USA
[39]James Madison University, Harrisonburg, Virginia 22807, USA
[40]Università di Ferrara, 44121 Ferrara, Italy
[41]Arizona State University, Tempe, Arizona 85287-1504, USA
[42]California State University, Dominguez Hills, Carson, California 90747, USA
[43]Edinburgh University, Edinburgh EH9 3JZ, United Kingdom
[44]Università di Genova, Dipartimento di Fisica, 16146 Genova, Italy

(Received 6 November 2017; revised manuscript received 5 December 2017; published 8 February 2018)

We measured the g_1 spin structure function of the deuteron at low Q^2, where QCD can be approximated with chiral perturbation theory (χPT). The data cover the resonance region, up to an invariant mass of $W \approx 1.9$ GeV. The generalized Gerasimov-Drell-Hearn sum, the moment Γ_1^d and the spin polarizability γ_0^d are precisely determined down to a minimum Q^2 of 0.02 GeV^2 for the first time, about 2.5 times lower than that of previous data. We compare them to several χPT calculations and models. These results are the first in a program of benchmark measurements of polarization observables in the χPT domain.

DOI: 10.1103/PhysRevLett.120.062501

For the last three decades, the spin structure of the nucleon has been actively studied experimentally and theoretically [1,2]. The reason is that spin degrees of freedom are uniquely sensitive to the details of the strong interaction that binds quarks into nucleons. The first challenge encountered by these studies was the "spin crisis": the discovery that the quark spins contribute less than expected to the proton spin [3]. The spin crisis brought the realization that spin sum rules could be used to address other challenging questions about quantum chromodynamics (QCD) [4] like quark confinement and how the low energy effective degrees of freedom of QCD (hadrons) are related to its fundamental ones (quarks and gluons).

This article reports the first precise measurement of the Q^2 evolution of the generalized Gerasimov-Drell-Hearn (GDH) integral [5,6] and of the spin polarizability γ_0 [7] on the deuteron at very low four-momentum transfer Q^2. Such a measurement allows us to test chiral perturbation theory (χPT)—a low Q^2 approximation of QCD—which has been challenged by earlier measurements of the GDH integral and of spin polarizabilities [8–14]. These measurements were dedicated, however, to study QCD's hadron-parton transition. Only their lowest Q^2 points (0.05 GeV^2 for H and D and 0.1 GeV^2 for ^{3}He) reached the χPT domain, and with limited precision. The results reported here are from the Jefferson Lab (JLab) CLAS EG4 experiment, dedicated to measure the proton, deuteron, and neutron polarized inclusive cross section at significantly lower Q^2 than previously measured. A complementary program exists in JLab's Hall A, dedicated to the neutron from ^{3}He [15] and to the transversely polarized proton [16].

An additional goal of EG4 was to assess the reliability of extracting neutron structure information from measurements on nuclear targets. The deuteron and ^{3}He complement each other for neutron information: nuclear binding effects in the deuteron are smaller than for ^{3}He, but to obtain the neutron information, a large proton contribution is subtracted. The proton contributions in ^{3}He are small, making polarized ^{3}He nearly a polarized neutron target. However, the tightly bound nucleons in ^{3}He have larger nuclear binding effects and non-nucleonic degrees of freedom may play a larger role.

Sum rules relate an integral over a dynamical quantity to a global property of the object under study. They offer stringent tests of the theories from which they originate. The Bjorken [17] and the GDH [5,6] sum rules are important examples. The latter was originally derived for photoproduction, $Q^2 = 0$, and links the helicity-dependent photoproduction cross sections σ_A and σ_P to the anomalous magnetic moment κ of the target:

$$\int_{\nu_0}^{\infty} \frac{\sigma_A(\nu) - \sigma_P(\nu)}{\nu} d\nu = -\frac{4\pi^2 S\alpha\kappa^2}{M^2}, \tag{1}$$

where M is the mass of the object, S its spin, α the QED coupling, ν the photon energy and ν_0 the photoproduction threshold. The A and P correspond to the cases where the photon spin is antiparallel and parallel to the object spin, respectively. For the deuteron, $S = 1$ and $-4\pi^2 S\alpha\kappa^2/M^2 = -0.6481(0)$ μb [18]. The GDH sum rule originates from a dispersion relation and a low energy theorem that are quite general and independent of QCD. The only assumption involves the convergence necessary to validate the dispersion relation. As such, the sum rule is regarded as a solid general prediction, and experiments at MAMI, ELSA, and LEGS [19] have verified it within about 7% precision for the proton. Verifying the sum rule on the neutron is more difficult since no free-neutron targets exist. Deuteron data taken at MAMI, ELSA, and LEGS cover up to $\nu = 1.8$ GeV [19] but have not yet tested the sum rule due to the delicate cancellation of the deuteron photodisintegration channel ($\approx$400 μb) with the other inelastic channels ($\approx$401 μb) [20].

In the midst of the "spin crisis," it was realized that the GDH integral could be extended to electroproduction to study the transition between the perturbative and nonperturbative domains of QCD [4]. A decade later, the sum rule itself was generalized [21,22]:

$$\Gamma_1(Q^2) = \int_0^{x_0} g_1(x, Q^2)dx = \frac{Q^2}{2M^2} I_1(Q^2), \qquad (2)$$

where g_1 is the first inclusive spin structure function, I_1 is the $\nu \to 0$ limit of the first covariant polarized VVCS amplitude, $x = Q^2/2M\nu$, and x_0 is the electroproduction threshold. The generalization connects the original GDH sum rule, Eq. (1), to the Bjorken sum rule [17].

The generalized GDH sum rule is valuable because it offers a fundamental relation for any Q^2. In the low and high Q^2 limits where Γ_1 can be related to global properties of the target, the sum rule tests our understanding of the nucleon spin structure. At intermediate Q^2 it has been used to test nonperturbative QCD calculations of Γ_1 such as the LFHQCD approach [23], phenomenological models of the nucleon structure [24] and, at lower Q^2, χPT calculations [25–27].

An ancillary result of the present low-Q^2 data is their extrapolation to $Q^2 = 0$ in order to check the sum rule on $\approx$(proton + neutron) [20] and on the neutron. Although the extrapolation adds an uncertainty to these determinations, the inclusive electron scattering used in this work sums all the reaction channels without the need to detect final state particles, unlike photoproduction that requires detecting each final state, with more associated systematic uncertainties.

The GDH and Bjorken sum rules involve the first moment of the spin structure functions. Other sum rules exist that employ higher moments such as the spin polarizability γ_0 sum rule [22]:

$$\gamma_0(Q^2) = \frac{16\alpha M^2}{Q^6} \int_0^{x_0} x^2 \left(g_1 - \frac{4M^2}{Q^2} x^2 g_2 \right) dx, \qquad (3)$$

where g_2 is the second spin structure function. An advantage of the polarizability is that the kinematic weighting highly suppresses the low-x contribution to the sum rule, which typically must be estimated with model input since it is inaccessible by experiment. For this reason, γ_0 provides a robust test of χPT, although it has a higher sensitivity to how data is extracted near the inelastic threshold. γ_0 has been measured at MAMI for $Q^2 = 0$ and at JLab on the proton, neutron and deuteron for $0.05 \leq Q^2 \leq 4$ GeV^2 [10–14].

The JLab data revealed unexpected discrepancies with χPT calculations for γ_0, its isovector and isoscalar components, and the generalized longitudinal-transverse spin polarizability δ_{LT}^n [10–13]. The data for γ_0 and Γ_1 typically agree with χPT calculations only for the lowest Q^2 points investigated ($Q^2 \lesssim 0.07$ GeV^2) and generally only with one type of χPT calculations: for a given observable, the results of Ref. [25] would agree and the ones of Ref. [26] would not, while the opposite occurs for another observable. Furthermore, the experimental and theoretical uncertainties of the first generation of experiments and calculations limited the usefulness of these comparisons. Conversely, $\Gamma_1^p - \Gamma_1^n$ was found to agree well with χPT [12]. No data on δ_{LT}^p exist although some are anticipated soon [16]. This state of affairs triggered a refinement of the χPT calculations [25–27] and a very low Q^2 experimental program.

The EG4 experiment took place in 2006 at JLab using the CLAS spectrometer in Hall B [28]. The aim was to measure g_1^p and g_1^d over an x range large enough to provide most of the generalized GDH integral, and over a Q^2 range covering the region where χPT should apply. The inclusive scattering of polarized electrons off longitudinally polarized protons or deuterons was the reaction of interest, but exclusive ancillary data were also recorded [29]. For the deuteron run, two incident electron beam energies were used, 1.3 GeV and 2.0 GeV. To cover the low angles necessary to reach the Q^2 values relevant to test χPT, a dedicated Cherenkov Counter (CC) was constructed and added to one of the CLAS spectrometer sectors. Furthermore, the target position was moved 1 m upstream of the nominal CLAS center and the toroidal magnetic field of CLAS bent electrons outward, yielding a minimum scattering angle of about 6°. This resulted in a coverage of $0.02 \leq Q^2 \leq 0.84$ GeV^2 and of invariant mass $W \leq 1.9$ GeV.

The polarized beam was produced by illuminating a strained GaAs cathode with a polarized diode laser. A Pockels cell flipped the beam helicity pseudorandomly at 30 Hz and a half wave plate was inserted periodically to provide an additional change of helicity sign to cancel possible false beam asymmetries. The beam polarization varied around $85 \pm 2\%$ and was monitored with a Møller polarimeter [28]. The beam current ranged between 1 and 3 nA.

The polarized deuteron target consisted of $^{15}ND_3$ ammonia beads held in a 1 K ^{4}He bath, and placed in a 5 T field

[30]. The target was polarized using dynamical nuclear polarization. The polarization was enhanced *via* irradiation with microwaves. The target polarization was monitored by a nuclear magnetic resonance (NMR) system and ranged between 30% and 45%. The polarization orientation was always along the beam direction. The NMR and Møller-derived polarizations were used for monitoring only, the product of the beam and target polarizations for the analysis being provided through the measured asymmetry of quasielastic scattering.

The scattered electrons were detected by the CLAS spectrometer. Besides the new CC used for data acquisition triggering and electron identification, CLAS contained three multilayer drift chambers that provided the momenta and charges of the scattered particles, time-of-flight counters and electromagnetic calorimeters (EC) for further particle identification. The trigger for the data acquisition system was provided by a coincidence between the new CC and the EC. Complementary data were taken with an EC-only trigger for efficiency measurements. Further information on EG4 can be found in Refs. [29,31].

The spin structure function g_1 was extracted in W and Q^2 bins from the measured difference in cross sections between antiparallel and parallel beam and target polarizations:

$$\frac{N^{\uparrow\Downarrow}(W,Q^2)}{\mathcal{L}P_bP_taQ_b^{\uparrow\Downarrow}} - \frac{N^{\uparrow\Uparrow}(W,Q^2)}{\mathcal{L}P_bP_taQ_b^{\uparrow\Uparrow}} = \Delta\sigma(W,Q^2), \qquad (4)$$

where "$\uparrow\Downarrow$" or "$\uparrow\Uparrow$" refers to beam spin and target polarization being antiparallel or parallel, respectively. N is the number of counts and Q_b is the corresponding integrated beam charge. $\mathcal{L}$ is a constant corresponding to the density of polarized target nuclei per unit area, P_bP_t is the product of the beam and target polarizations and $a(W,Q^2)$ is the detector acceptance, which also accounts for detector, trigger, and cut efficiencies. $\Delta\sigma$ is the polarization dependent inclusive cross section difference in a given (W,Q^2) bin and can be written as a linear combination of g_1 and g_2, see Refs. [1,2]. Only polarized material contributes to $\Delta\sigma$, which is advantageous due to the dilution factor of the polarized targets used by EG4.

The product of the polarized luminosity, beam and target polarizations, P_bP_t, and the overall electron detection efficiency was determined by comparing the measured yield difference in the quasielastic region, $0.9 < W < 1$ GeV, with the calculated values. An event generator based on RCSLACPOL [32], with up-to-date models of structure functions and asymmetries for inelastic scattering from deuterium [14], was used to generate events according to the fully radiated cross section. The events were followed through a full simulation of the CLAS spectrometer based on a GEANT-3 simulation package. Thus, the simulated events were analyzed in the same way as the measured data, thereby accounting for the bin-to-bin variation of acceptance and efficiency [Eq. (4)]. A comparison between the simulated and the measured data in a given Q^2 bin is shown in Fig. 1. Any deviation between the simulation and the experimental results can be due to two possible sources: (1) A genuine difference between the g_1 models and the true value within that bin, and (2) the systematic deviations of all other ingredients entering the simulation from their correct values: this includes backgrounds and detector efficiencies and distortions, models for other structure functions (F_2, R) and asymmetries (A_2), and radiative effects. To extract $g_1(W,Q^2)$ from our measured data, we determined the amount δg_1, by which the model for g_1 had to be varied in a given bin to fully account for the difference between measured and simulated yield difference. The systematic uncertainty on g_1 due to each of the sources (2) above was determined by varying one of the ingredients within their reasonable uncertainties and extracting the corresponding impact on g_1 accordingly. It is important to understand that although a model is used for obtaining g_1, there is little model dependence in the results reported here.

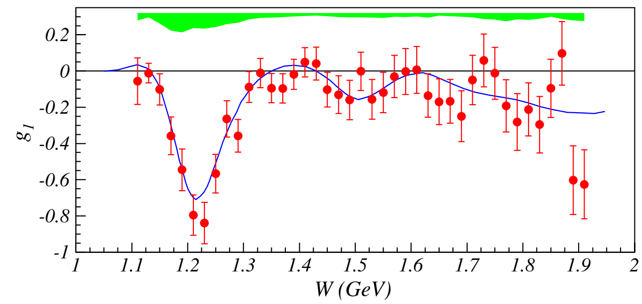

FIG. 1. Example of extracted $g_1^d(W)$ vs invariant mass W (circles), together with the nominal value of the parameterization used for its extraction (line). The large negative peak corresponds to the $\Delta(1232)3/2^+$ resonance. The error bars give the statistical uncertainty and the band is the total systematic uncertainty. The data are for $\langle Q^2\rangle = 0.1$ GeV^2.

Cuts were used for particle identification, to reject events not originating from the target, to select detector areas of high acceptance and high detector efficiency, where the detector simulation reproduces well the data [31]. Corrections were applied for contaminations from π^- (typically less than 1%) and from secondary electrons produced from photons or π^0 decay (nearly always less than 3%). Quality checks were performed, including detector and yield stability with time. Vertex corrections to account for the beam raster, any target-detector misalignments, and toroidal field mapping inaccuracies, were determined and applied. Electron energy losses by ionization in the target or detector material were corrected for, as well as bremsstrahlung and other radiative corrections. This was done using the same method as in Refs. [10,13,14].

Systematic uncertainties are typically of the order 10% of the extracted values for $g_1(x,Q^2)$ and nearly always smaller than statistical uncertainties. They are dominated by the overall normalization uncertainty (about 7–10%, depending on the kinematic bin, and largely correlated), model uncertainties for unmeasured quantities (up to 10% in a few kinematic bins, but normally smaller), and radiative corrections and kinematic uncertainties (up to 5% near threshold but much smaller elsewhere). These latter are mostly point-to-point uncorrelated. The model uncertainties were estimated by modifying the parameters controlling $g_1(x, Q^2)$ and $g_2(x, Q^2)$. The calculation and comparison of these contributions are detailed in Ref. [31].

The complete g_1^d data set and related moments are provided in tables as Supplemental Material [33]. The integrals in Eqs. (2)–(3) are formed by integrating the data over the $x_{\mathrm{min}} < x < x_0$ range, where x_{min} is the lowest x reached by the experiment for a given Q^2 bin. For the lowest Q^2 bin, 0.020 GeV^2, $x_{\mathrm{min}} = 0.0073$, and for the largest Q^2 bin considered for integration, 0.592 GeV^2, $x_{\mathrm{min}} = 0.280$. The data are supplemented by the model to cover the integration range $0.001 < x < x_{\mathrm{min}}$ and the threshold contribution ($1.07 < W < 1.15$ GeV) at high x. There, the model is used rather than data to avoid quasielastic scattering and radiative tail contaminations [31].

The integral $\Gamma_1^d(Q^2)$ is shown in Fig. 2. The original GDH sum rule provides the derivative of Γ_1 at $Q^2 = 0$. The low-x correction is small. The full integral (solid squares) agrees with the previous CLAS EG1b experiment [14], but the minimum Q^2 is 2.5 times lower. The statistical uncertainty of EG4 is improved over EG1b by about a factor of 4 at the lowest Q^2 points, and thus, it allows for a more stringent test of χPT. The Lensky *et al.* χPT calculation [27], which supersedes the earlier calculations

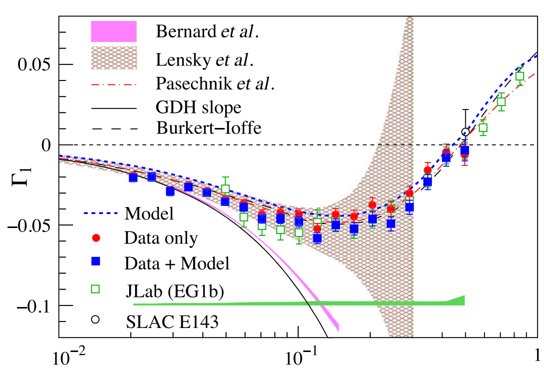

FIG. 2. The first moment $\Gamma_1^d(Q^2)$. The solid circles are the EG4 data integrated over the covered kinematics. The fully integrated Γ_1^d, using a model to supplement data, is shown by the solid squares. The error bars are statistical. The systematic uncertainty is given by the horizontal band. The open symbols show data from the CLAS EG1b [14] and SLAC E143 [32] experiments. The other bands and lines show various models and χPT calculations as described in the text. The short-dash line (Model) does not include the EG4 data, to reveal the new knowledge gained.

in Ref. [26], agrees with the data. The most recent Bernard *et al.* χPT calculation [25] agrees with the few lowest Q^2 points. The Pasechnik *et al.* and Burkert-Ioffe parametrizations [24] describe the data well.

The data can also be integrated to form the related moment $\bar{I}_{TT}^d(Q^2)$ [6] extrapolated to $Q^2 = 0$ and compared with the original sum rule expectation that $I_{TT}(0) = -\kappa^2/4$. Accounting for the deuteron D state and ignoring two body breakup and coherent channels, the GDH sum rule predicts $\bar{I}_{TT}^d = (1 - 3\omega_D/2)(I_{TT}^p + I_{TT}^n) = -1.574 \pm 0.026$, with $\omega_D = 0.056 \pm 0.01$ [34]. We extrapolated to $Q^2 = 0$ the data below $Q^2 = 0.06$ GeV^2, which average at $\langle Q^2 \rangle = 0.045$ GeV^2. To this end, we used the (small) Q^2 dependence of the Lensky *et al.* calculation [27], since it agrees very well with the data. We find $\bar{I}_{TT}^{d\,\mathrm{exp}}(0) = -1.724 \pm 0.027(\mathrm{stat}) \pm 0.050(\mathrm{syst})$. This is 10%, or 1.5σ, away from the sum rule prediction of -1.574 ± 0.026. This can be compared with the MAMI and ELSA measurement with real photons: $\bar{I}_{TT}^{d\,\mathrm{exp}}(0) = -1.986 \pm 0.008(\mathrm{stat}) \pm 0.010(\mathrm{syst})$ integrated over $0.2 < \nu < 1.8$ GeV (the systematic uncertainties here do not include any low and large ν contributions) [19]. Using the proton GDH sum rule world data [19], we deduce the neutron GDH integral $I_{TT}^{n\,\mathrm{exp}}(0) = -0.955 \pm 0.040(\mathrm{stat}) \pm 0.113(\mathrm{syst})$, which agrees within uncertainties with the sum rule expectation $I_{TT}^{n\,\mathrm{theo}}(0) = -0.803$.

Finally, the generalized spin polarizability $\gamma_0(Q^2)$ can be formed from Eq. (3) and is shown in Fig. 3. The MAID prediction, a multipole analysis of photo- and electroproduced resonance data up to $W = 2$ GeV [35], is relevant since the low-x contribution, not included in MAID, is largely suppressed. The χPT calculations differ markedly. The full γ_0 from EG4 (solid squares) agrees with the Bernard *et al.* χPT calculation [25], and it disagrees with the Lensky *et al.* χPT calculation [27] and with the MAID model below 0.07 GeV^2.

To conclude, we report the first precise measurement of the Q^2 evolution of Γ_1^d and of the spin polarizability γ_0 on the deuteron in the $0.02 < Q^2 < 0.59$ GeV^2 domain. The

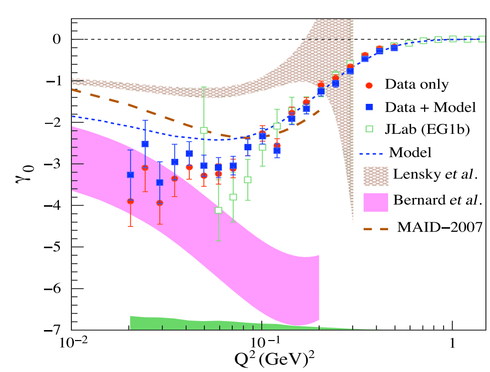

FIG. 3. The generalized spin polarizability $\gamma_0(Q^2)$. See Fig. 2 for legends and theoretical calculations.

data reach a minimal Q^2 2.5 times lower than that of previously available data, with much improved precision. The degree of agreement of the different χPT methods varies with the observable: the Bernard *et al.* calculations are more successful with γ_0, while the Lensky *et al.* ones describe Γ_1 well. Thus, no single method successfully describes both observables, and while chiral calculations are reaching higher precision, a satisfactory description of spin observables remains challenging. The phenomenological models of Pasechnik *et al.* and Burkert-Ioffe agree well with the GDH data. The MAID model disagrees with the γ_0 data for $Q^2 \leq 0.07$ GeV^2. Our data, extrapolated to $Q^2 = 0$ to check the GDH sum rule for the neutron, agree with it to within 20%, or about 1.0σ.

The program of providing benchmark polarization observables for χPT will be completed when the proton EG4 data become available, as well as the longitudinally and the transversally polarized data on the neutron (^{3}He) [15] and proton [16] from JLab's Hall A.

This work was supported by the U.S. Department of Energy (DOE), the U.S. National Science Foundation, the U.S. Jeffress Memorial Trust, the Physics and Astronomy Department and the Office of Research and Economic Development at Mississippi State University, the United Kingdom Science and Technology Facilities Council (STFC), the Italian Istituto Nazionale di Fisica Nucleare, the French Institut National de Physique Nucléaire et de Physique des Particules, the French Centre National de la Recherche Scientifique, and the National Research Foundation of Korea. This material is based upon work supported by the U.S. Department of Energy, Office of Science, Office of Nuclear Physics under Contract No. DE-AC05-06OR23177.

[*]deurpam@jlab.org

[1] S. E. Kuhn, J.-P. Chen, and E. Leader, Prog. Part. Nucl. Phys. **63**, 1 (2009); J. P. Chen, Int. J. Mod. Phys. E **19**, 1893 (2010).

[2] For a recent review, see C. A. Aidala, S. D. Bass, D. Hasch, and G. K. Mallot, Rev. Mod. Phys. **85**, 655 (2013).

[3] J. Ashman *et al.* (European Muon Collaboration), Phys. Lett. B **206**, 364 (1988).

[4] M. Anselmino, B. L. Ioffe, and E. Leader, Yad. Fiz. **49**, 214 (1989) [Sov. J. Nucl. Phys. **49**, 136 (1989)].

[5] S. B. Gerasimov, Yad. Fiz. **2**, 598 (1965) [Sov. J. Nucl. Phys. **2**, 430 (1966)]; S. D. Drell and A. C. Hearn, Phys. Rev. Lett. **16**, 908 (1966); M. Hosoda and K. Yamamoto, Prog. Theor. Phys. **36**, 425 (1966).

[6] For a review of the sum rule and its verification, see: K. Helbing, Prog. Part. Nucl. Phys. **57**, 405 (2006).

[7] P. A. M. Guichon, G. Q. Liu, and A. W. Thomas, Nucl. Phys. **A591**, 606 (1995).

[8] M. Amarian *et al.*, Phys. Rev. Lett. **89**, 242301 (2002); **92**, 022301 (2004); A. Deur *et al.*, Phys. Rev. Lett. **93**, 212001 (2004).

[9] K. Slifer *et al.* Phys. Rev. Lett. **101**, 022303 (2008).

[10] J. Yun *et al.* (CLAS Collaboration), Phys. Rev. C **67**, 055204 (2003); R. Fatemi *et al.* (CLAS Collaboration), Phys. Rev. Lett. **91**, 222002 (2003); K. V. Dharmawardane *et al.* (CLAS Collaboration), Phys. Lett. B **641**, 11 (2006); Y. Prok *et al.* (CLAS Collaboration), Phys. Lett. B **672**, 12 (2009).

[11] M. Amarian *et al.* (E94010 Collaboration), Phys. Rev. Lett. **93**, 152301 (2004).

[12] A. Deur *et al.*, Phys. Rev. D **78**, 032001 (2008).

[13] R. G. Fersch *et al.* (CLAS Collaboration), Phys. Rev. C **96**, 065208 (2017).

[14] N. Guler *et al.* (CLAS Collaboration), Phys. Rev. C **92**, 055201 (2015).

[15] V. Sulkosky *et al.* (to be published).

[16] R. Zielinski *et al.* (to be published).

[17] J. D. Bjorken, Phys. Rev. **148**, 1467 (1966); Phys. Rev. D **1**, 1376 (1970).

[18] C. Patrignani *et al.* (Particle Data Group), Chin. Phys. C **40**, 100001 (2016).

[19] J. Ahrens *et al.* (GDH and A2 Collaborations), Phys. Rev. Lett. **87**, 022003 (2001); **97**, 202303 (2006); H. Dutz *et al.* (GDH Collaboration), Phys. Rev. Lett. **91**, 192001 (2003); **93**, 032003 (2004); **94**, 162001 (2005); S. Hoblit *et al.* (LSC Collaboration), Phys. Rev. Lett. **102**, 172002 (2009).

[20] In this Letter, we exclude most of the deuteron break-up channel by requiring $W = \sqrt{M^2 + 2M\nu - Q^2} > 1.15$ GeV. In that case, the integrals are close to the incoherent sums of the corresponding integrals for the proton and the neutron, modified by the deuteron D state correction factor.

[21] X. D. Ji and J. Osborne, J. Phys. G **27**, 127 (2001).

[22] D. Drechsel, B. Pasquini, and M. Vanderhaeghen, Phys. Rep. **378**, 99 (2003).

[23] S. J. Brodsky, G. F. de Teramond, and A. Deur, Phys. Rev. D **81**, 096010 (2010).

[24] V. Burkert and Z. Li, Phys. Rev. D **47**, 46 (1993); V. D. Burkert and B. L. Ioffe, Phys. Lett. B **296**, 223 (1992); Zh. Eksp. Teor. Fiz. **105**, 1153 (1994); [J. Exp. Theor. Phys. **78**, 619 (1994)]; R. S. Pasechnik, J. Soffer, and O. V. Teryaev, Phys. Rev. D **82**, 076007 (2010).

[25] V. Bernard, N. Kaiser, and Ulf-G. Meissner, Phys. Rev. D **48**, 3062 (1993); V. Bernard, T. R. Hemmert, and Ulf-G. Meissner, Phys. Lett. B **545**, 105 (2002); V. Bernard, T. R. Hemmert, and Ulf-G. Meissner, Phys. Rev. D **67**, 076008 (2003); V. Bernard, E. Epelbaum, H. Krebs, and Ulf-G. Meissner, Phys. Rev. D **87**, 054032 (2013).

[26] X. D. Ji, C. W. Kao, and J. Osborne, Phys. Lett. B **472**, 1 (2000); Phys. Rev. D **61**, 074003 (2000); C. W. Kao, T. Spitzenberg, and M. Vanderhaeghen, Phys. Rev. D **67**, 016001 (2003).

[27] V. Lensky, J. M. Alarcon, and V. Pascalutsa, Phys. Rev. C **90**, 055202 (2014).

[28] B. A. Mecking *et al.*, Nucl. Instrum. Methods Phys. Res., Sect. A **503**, 513 (2003).

[29] X. Zheng *et al.* (CLAS Collaboration), Phys. Rev. C **94**, 045206 (2016).

[30] D. G. Crabb and D. B. Day, Nucl. Instrum. Methods Phys. Res., Sect. A **356**, 9 (1995); C. D. Keith *et al.*, Nucl. Instrum. Methods Phys. Res., Sect. A **501**, 327 (2003).

[31] K. Adhikari, Ph.D. dissertation, Old Dominion University 2013. www.jlab.org/Hall-B/general/thesis/Adhikari_thesis.pdf.

[32] K. Abe *et al.* (E143 Collaboration), Phys. Rev. D **58**, 112003 (1998).

[33] See Supplemental Material at http://link.aps.org/supplemental/10.1103/PhysRevLett.120.062501 for data for the moments γ_1^d, I_{TT}^d, and γ_0^d are provided in Table I. The data on the spin structure function g_1^d and the ratio A_1^d/F_1^d are provided in Table II.

[34] M. Lacombe, B. Loiseau, J. M. Richard, R. Vinh Mau, J. Côté, P. Pirès, and R. de Tourreil, Phys. Rev. C **21**, 861 (1980); R. Machleidt, K. Holinde, and C. Elster, Phys. Rep. **149**, 1 (1987); M. J. Zuilhof and J. A. Tjon, Phys. Rev. C **22**, 2369 (1980); K. Kotthoff, R. Machleidt, and D. Schutte, Nucl. Phys. **A264**, 484 (1976); B. Desplanques, Phys. Lett. B **203**, 200 (1988).

[35] D. Drechsel, S. Kamalov, and L. Tiator, Nucl. Phys. **A645**, 145 (1999).